

Analysis and Design of CMOS Coupled Multivibrators

João Casaleiro, Hugo F. Lopes, Luis B. Oliveira, and Igor Filanovsky

Abstract—In this paper a wideband MOS quadrature oscillator constituted by two multivibrators is presented. Two different forms of coupling, named here as soft and hard, are investigated. Simulations are performed in a 0.13 μm CMOS technology to obtain the tuning range, the synchronization transients, and the influence of mismatches in timing capacitors and charging currents on synchronization. It is found that hard coupling reduces the quadrature error (about 1° , with 5% mismatches in timing capacitors and charging currents) and results in a low phase-noise (about 2 dB improvement) with respect to soft coupling. Either a single multivibrator or coupled multivibrators can be locked to an external synchronizing harmonic frequency, and the locking range is investigated by simulations. The simulations are done for oscillators covering the WTMS frequency bands.

Index Terms—CMOS oscillator, multivibrator, quadrature outputs, van der Pol oscillator, WMTS applications.

I. INTRODUCTION

QUADRATURE oscillators are key blocks in the design of modern transceivers. In recent years, significant research efforts have been invested in the study of low area and low cost oscillators, with accurate quadrature outputs [1 - 7].

The circuit presented in this paper is intended for use in the Wireless Medical Telemetry Service (WMTS), which establishes wireless communication between an externally worn medical device and other equipment [8]. There are three frequency bands allocated to WMTS: 608 - 614 MHz, 1395 - 1400 MHz and 1427 - 1432 MHz. With the proposed circuit we intend to cover all the bands allowed for these applications.

Emitter and source-coupled multivibrators are used frequently as voltage-controlled oscillators (VCOs) [9-11]. These multivibrators may be coupled [12] to produce quadrature oscillators.

This work was supported by the Portuguese Foundation for Science and Technology (CTS-UNINOVA and INESC-ID multiannual funding and project LEADER (PTDC/EEA-ELC/69791/2006)) through the PIDDAC Program funds.

J. Casaleiro, H. Lopes, and L. B. Oliveira are with the Department of Electrical Engineering, Faculty of Sciences and Technology, and with the Center of Technology and Systems (CTS-UNINOVA), Universidade Nova de Lisboa, 2829-516 Caparica, Portugal (e-mail: Loliveira@fct.unl.pt).

L. B. Oliveira is also with the R&D IC unit of INESC-ID, 1000 Lisbon, Portugal.

I. Filanovsky is with University of Alberta, Edmonton, Alberta, Canada (email: igor@ece.ualberta.ca)

In this paper (Section II) we show why the chosen multivibrator is the most suitable for coupling. In Section III the MOS quadrature oscillator is described. Section IV gives simulation results in a 0.13 μm CMOS technology for the tuning range, the synchronization transients, and the influence of mismatches of timing capacitors and charging currents on synchronization. Section V gives some results for external synchronization. A discussion and some conclusions are given in Section VI.

II. SINUSOIDAL AND RELAXATION OSCILLATIONS

The bipolar version of the circuit in Fig. 1 (a) was widely used in VCOs [13, 14] and the circuit was considered as a very stable and reliable multivibrator. The tendency to operate at higher frequencies using modern CMOS technologies confirmed that this circuit is able to have sinusoidal operation as well, and the relaxation operation should be considered as the limit form of such operation. As shown below, this circuit is a van der Pol oscillator, for which the transition from sinusoidal to relaxation operation is the natural process connected with continuous change of one of the circuit parameters [11]. Because this circuit has both kinds of operation we will use the words “oscillator” and “multivibrator” rather indiscriminately.

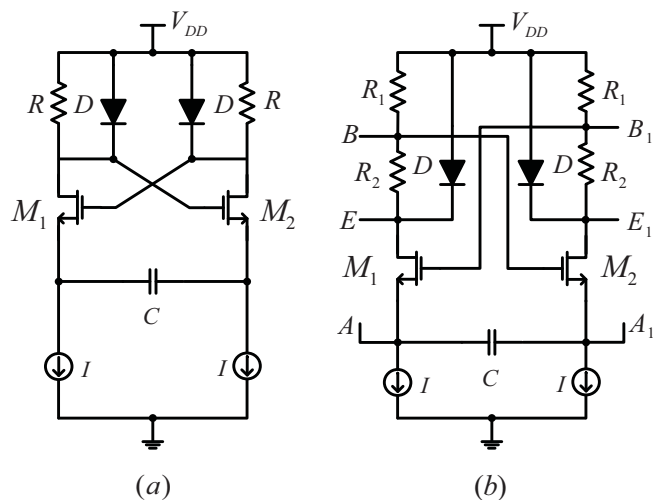


Figure 1. Current-controlled multivibrator (a) and its modification (b).

Assume that the oscillation amplitude developed on resistors R is so small that the diodes are OFF. Using simplified models (controlled transconductance and gate-source capacitance) for transistors M_1 and M_2 it is possible to show that the capacitor C "sees" the impedance

$$z_{in} = \frac{(C_{gs}s + G)(g_{m1} + g_{m2})}{G} - \frac{2}{g_{m1}g_{m2}G} \quad (1)$$

where $G = 1/R$. The oscillator characteristic equation is

$$(1/Cs) + z_{in} = 0 \quad (2)$$

Substituting (1) in (2) one obtains that

$$s^2 + \frac{1}{RC_{gs}} \left(1 - 2R \frac{g_{m1}g_{m2}}{g_{m1} + g_{m2}} \right) s + \frac{g_{m1}g_{m2}}{RCC_{gs}(g_{m1} + g_{m2})} = 0 \quad (3)$$

When the oscillation starts one may consider that $g_{m1} = g_{m2} = g_{m0} = \sqrt{2\mu_n C_{ox}(W/L)I}$, and (3) can be rewritten as

$$s^2 + \frac{1}{RC_{gs}}(1 - Rg_{m0})s + \frac{g_{m0}}{2RCC_{gs}} = 0 \quad (4)$$

The oscillations will start if the roots of this equation are located in the right half of the s -plane. This requires that

$$g_{m0} > 1/R \quad (5)$$

The oscillations will have the frequency

$$\omega_0 = \sqrt{g_{m0}/(2RCC_{gs})} \quad (6)$$

The roots of (4) are

$$s_{1,2} = \frac{g_{m0}R - 1}{2RC_{gs}} \pm \sqrt{\left(\frac{g_{m0}R - 1}{2RC_{gs}} \right)^2 - \frac{g_{m0}}{2RCC_{gs}}} \quad (7)$$

If C varies and all other parameters are constant, the roots move in the right half of the s -plane only. For small values of C they are complex-conjugate and located in the vicinity of $j\omega$ -axis. The oscillator has quasi-sinusoidal oscillations. With increase of C they move towards the positive real axis. The oscillations become more and more distorted. When $C = (2C_{gs}g_{m0}R)/(g_{m0}R - 1)^2$ the roots are positive real axis, and one may consider that the circuit has now relaxation oscillations. With further increase of C the roots move along positive real axis arriving to the final values of $s_1 = 0$ and $s_2 = (Rg_{m0} - 1)/(rC_{gs})$. The circuit oscillations are closer and closer to relaxation oscillations with discontinuous waveform. The transition from sinusoidal to relaxation oscillations is smooth with a gradual increase of distortions in the waveform [10] and specific amplitude limiting.

Let us do the approximation

$$\frac{g_{m1}g_{m2}}{g_{m1} + g_{m2}} \approx \frac{g_{m0}}{2} \left[1 - \left(\frac{i}{\sqrt{2}I} \right)^2 \right] \quad (8)$$

in the damping term of (3), and leave the frequency term the same as in (4). Here i is the capacitor current. Then, one can write for this current the differential equation

$$\frac{d^2i}{dt^2} + \frac{1}{RC_{gs}} \left\{ 1 - Rg_{m0} \left[1 - \left(\frac{i}{\sqrt{2}I} \right)^2 \right] \right\} \frac{di}{dt} + \omega_0^2 i = 0 \quad (9)$$

Introducing the normalized variable $x = i/(\sqrt{2}I)$ and using the notation $\delta_0 = (Rg_{m0} - 1)/(2RC_{gs})$ and $\delta_2 = g_{m0}/(2C_{gs})$, one reduces this equation to the standard van der Pol form

$$\frac{d^2x}{dt^2} - 2(\delta_0 - \delta_2 x^2) \frac{dx}{dt} + \omega_0^2 x = 0 \quad (10)$$

The solution of this equation for small distortions is

$$x = 2\sqrt{\delta_0/\delta_2} \sin \omega_0 t = 2\sqrt{1 - (1/Rg_{m0})} \sin \omega_0 t \quad (11)$$

The amplitude of the voltage between the drain resistors (the usual points of measurements) will be

$$V_{dm} = 4\sqrt{2}I\sqrt{1 - (1/Rg_{m0})} \quad (11)$$

If this amplitudes increases (say, if I increases as a result of tuning) the diodes eventually limit the amplitude. When the circuit moves to relaxation oscillation (at lower frequency) then the amplitude limiting by the diodes is dominating. The frequency may be approximated as

$$f_0 \approx I/(4V_{BE(ON)}C) \quad (12)$$

where $V_{BE(ON)} \approx 0.5$ V (MOS diodes) is the voltage drop on the diode-connected transistors D .

Due to the smooth transition from sinusoidal to relaxation oscillations and the existence of amplitude stabilization mechanisms, the frequency tuning range may be very wide [13 - 15]. It can be further increased by the modification shown in Fig. 1 b that allows higher oscillation frequencies, and is suitable for coupling two multivibrators in a quadrature oscillator. The voltage amplitude at the timing capacitor is now lower, but the oscillation frequency is

$$f_0 \approx I/\{4V_{BE(ON)}R_1/[(R_1 + R_2)C]\} \quad (13)$$

To obtain a quadrature oscillator one couples two similar oscillators using differential pairs [12, 16]. The inputs of the coupling differential pairs should be connected to the timing capacitors (at A and A₁). Their outputs can be connected either to nodes B and B₁ or E and E₁. A source with incremental current I_c injected at node B will create an incremental voltage V_b

$$V_b \approx (I_c R_1 R_2)/(R_1 + R_2) \quad (14)$$

(assuming that $r_d \ll R_2$, where r_d is the diode dynamic resistance). If I_c is injected at node E then V_b will be reduced to

$$V_b \approx (I_c R_1 r_d)/(R_1 + R_2) \quad (15)$$

assuming that $r_d \ll R_1 + R_2$.

The coupling at E and E₁, is called here “soft coupling”; at the divider taps B and B₁, it is called “hard coupling”. If R₁ + R₂ is constant the maximum coupling is achieved for R₁ ≈ R₂.

III. QUADRATURE OSCILLATOR

To obtain a quadrature oscillator one connects two multivibrators using two coupling differential pairs. Fig. 2 shows the “hard coupling” case. The synchronization mechanism is similar to that described for the coupling of unmodified multivibrators [16]: the coupling current changes the gate voltages of M₁ and M₂.

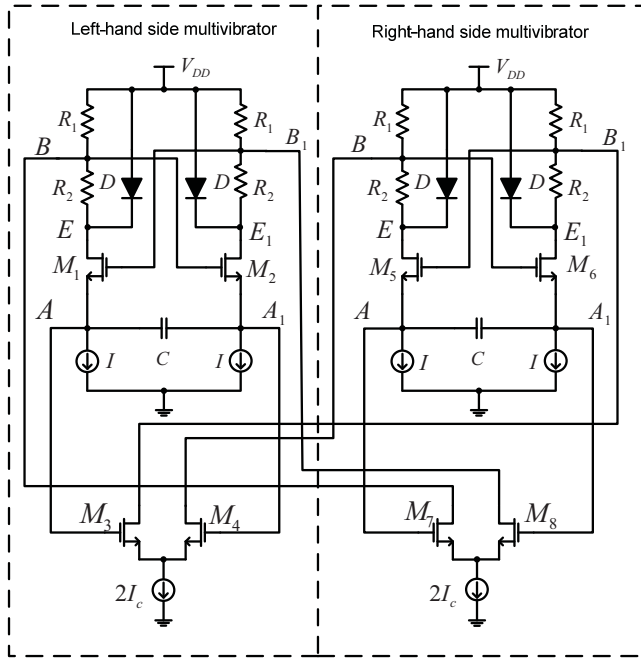


Figure 2. Quadrature current-controlled oscillator with “hard” coupling.

If the coupling current is low in comparison with the tuning current, its influence on the oscillation frequency is very weak. However, this current is able to change the switching time of the transistors M₁ and M₂, and this leads to synchronous oscillation of the constituent multivibrators. This minimizes the influence of noise sources in the switching point, which results in a reduction of the oscillator phase-noise and jitter. The synchronous frequency is approximately given by (13).

The synchronization theory of oscillations in the coupled system with relaxation oscillations is still under development, and we will give the results of simulations, thus, creating the basis for this theory.

IV. SIMULATION RESULTS

The circuit shown in Fig. 2 is simulated using 130 nm MOS technology. The transistors and resistor sizing are equal for both bands mentioned earlier, as well as the supply voltage (1.2 V). For the lower band the timing capacitor is C = 1.8 pF, and for the other band C = 400 fF. Other values are as

follows: R₁ = R₂ = R = 250 Ω, transistors M₁, M₂, M₅ and M₆ have W = 80 μm and L = 300 nm, M₃, M₄, M₇ and M₈ have W = 100 μm and L = 300 nm. The diode-connected transistors have W = 30 μm and L = 300 nm. The coupling current (I_c) is equal to 0.5 mA. Diode-connected PMOS transistors are used, because their temperature characteristics are better than those of NMOS devices.

The oscillator tuning characteristics are obtained by changing the tuning current (I) and the timing capacitor. Simulation results for MOS quadrature oscillators using the traditional “soft” coupling and the new “hard” coupling are presented in Figs. 3 and 4.

The characteristics of Fig. 3 are nearly linear after I = 0.5 mA, which is equal to the value of the coupling current I_c. If the tuning current is lower than the coupling current, the later will have a strong influence on the frequency. This means that, for low tuning currents, the switching times of transistors M₁, M₂, M₅ and M₆ must be taken into account. Hence both currents influence the oscillation period. In the quasi-linear zone these switching times can be neglected [13].

Fig. 4 is obtained by reducing the capacitance C = 400 fF. This causes a decrease of the capacitor charging time and the increase of the oscillation frequency.

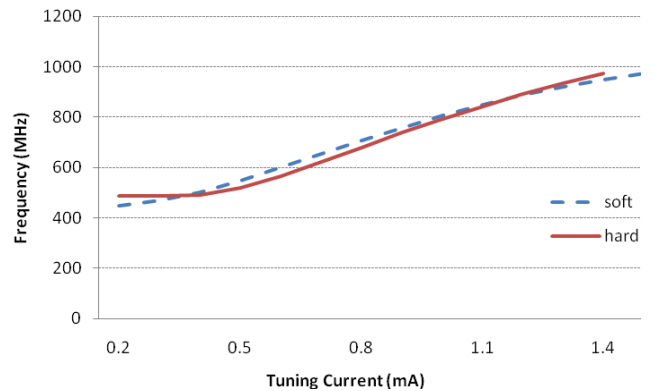


Figure 3. Tuning characteristic for 2I_c = 0.5 mA.

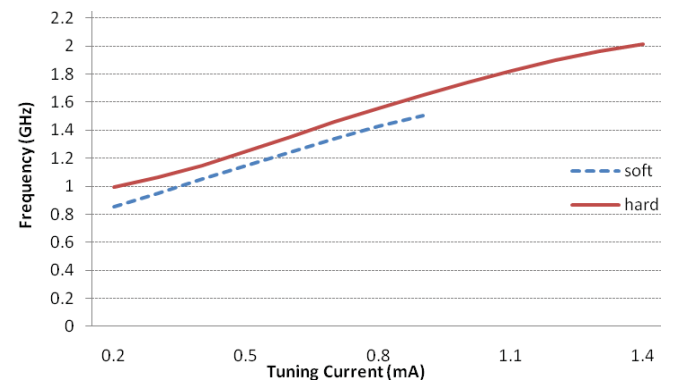


Figure 4. Tuning characteristic for 2I_c = 0.5 mA.

Figs. 5 and 6 show the output waveforms at 600 MHz and 1.4 GHz, respectively. Although one could expect a square wave at the output, that doesn’t happen due to the “soft” operation of the limiting diodes and the filtering of higher harmonics caused by the parasitic capacitances of the

transistors. These parasitics are also responsible for the deviation from linearity at high tuning currents in Figs. 3 and 4.

The oscillator phase-noise is -119.5 dBc/Hz @ 10 MHz offset for “soft” and -121.6 dBc/Hz @ 10 MHz offset for “hard” coupling (as shown in Fig. 7), for the 600 MHz band. For the 1.4 GHz band the oscillator phase-noise is -114.2 dBc/Hz @ 10 MHz offset for “soft” and -117.6 dBc/Hz @ 10 MHz offset for “hard” coupling. Thus, in both frequency bands, we observe a significant reduction of phase-noise for hard coupling.

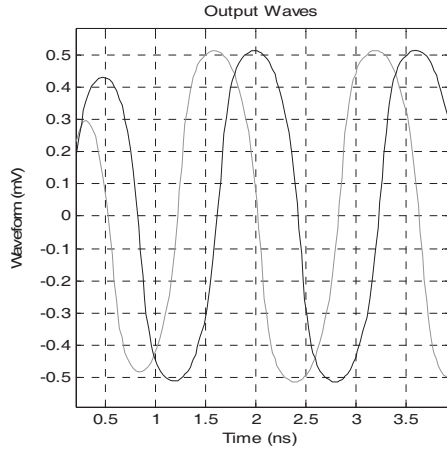


Figure 5. Output waveforms (600 MHz).

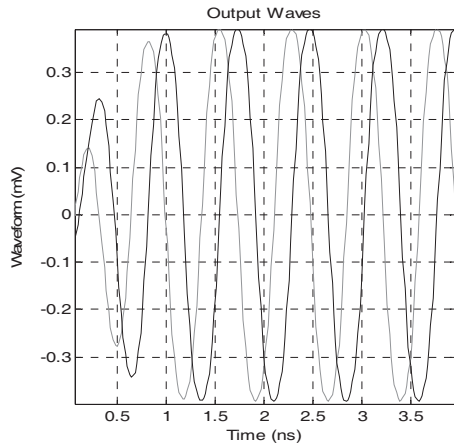


Figure 6. Output waveforms (1.4 GHz).

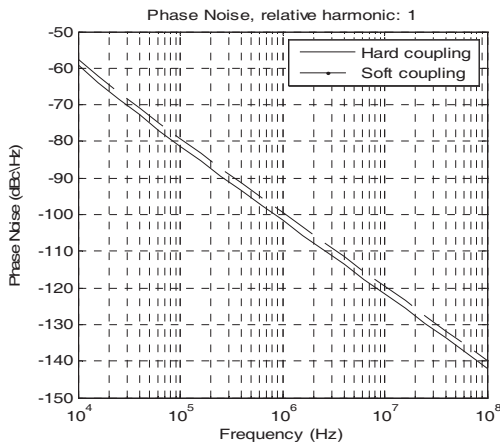


Figure 7. Oscillator phase-noise (“hard” coupling – 600 MHz).

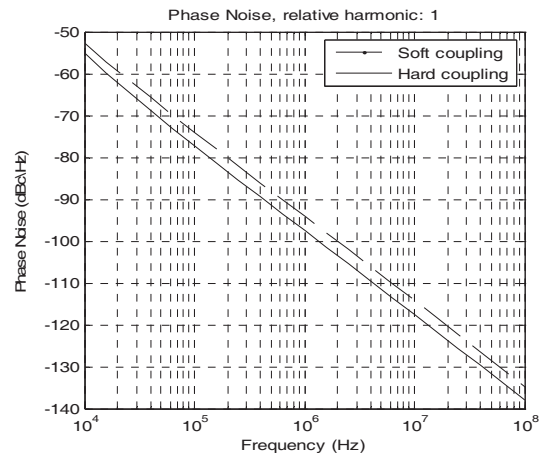


Figure 8. Oscillator phase-noise (“hard” coupling – 1.4 GHz).

Tables I and II show the influence of mismatches in the timing capacitances for “soft” and “hard” coupling for 600 MHz and 1.4 GHz, respectively. There is no oscillation for low values of the “soft” coupling current. In general the “hard” coupling provides significant lower phase error (about 1°) than the “soft” coupling. In Tables III and IV when the frequency mismatch starts to decrease reaching a value close to zero, the “soft” coupling starts to have reduced phase error, when compared to “hard” coupling. For a mismatch of 1% of the capacitances, the phase error is below 0.1° for all currents.

TABLE I. EFFECT OF 5% MISMATCHES IN CAPACITANCES (600 MHz)

$2 I_C$ (mA)	Soft coupling		Hard Coupling	
	Δf (MHz)	Phase error (°)	Δf (MHz)	Phase error (°)
0.1	53.85	10.28	12.27	7.95
0.2	45.21	5.19	12.49	4.22
0.3	34.35	3.23	11.62	2.97
0.4	21.93	2.38	10.44	2.15
0.5	8.22	1.91	8.95	1.66
0.6	6.64	1.62	7.44	1.61
0.7	22.24	1.33	5.92	1.39
0.8	38.43	0.99	4.41	1.17
0.9	54.82	0.95	2.76	0.95

TABLE II. EFFECT OF 5% MISMATCHES IN CAPACITANCES (1.4 GHz)

$2 I_C$ (mA)	Soft coupling		Hard Coupling	
	Δf (MHz)	Phase error (°)	Δf (MHz)	Phase error (°)
0.1	No oscillation		71.86	1.54
0.2	No oscillation		59.49	1.59
0.3	25.19	0.92	46.28	1.09
0.4	20.87	0.86	32.12	0.76
0.5	13.43	0.84	17.33	0.57
0.6	3.56	0.93	2.33	0.4
0.7	8.16	1.02	12.54	0.34
0.8	21.03	1.09	26.96	0.33
0.9	34.51	1.2	40.74	0.29

TABLE III. EFFECT OF 10% MISMATCHES IN CAPACITANCES (600 MHz)

$2 I_C$ (mA)	Soft coupling		Hard Coupling	
	Δf (MHz)	Phase error (°)	Δf (MHz)	Phase error (°)
0.1	59.28	21.23	19.66	15.9
0.2	52.33	9.77	20.31	8.22
0.3	41.63	6.29	19.68	5.7
0.4	29.24	4.5	18.44	4.37
0.5	15.59	3.59	16.98	3.61
0.6	0.83	2.71	15.49	3.12
0.7	14.66	2.19	14	2.77
0.8	30.83	1.84	12.5	2.48
0.9	47.23	1.37	10.97	2.26

TABLE IV. EFFECT OF 10% MISMATCHES IN CAPACITANCES (1.4 GHz)

$2 I_C$ (mA)	Soft coupling		Hard Coupling	
	Δf (MHz)	Phase error (°)	Δf (MHz)	Phase error (°)
0.1	No oscillation		88.93	5.69
0.2			75.18	4.38
0.3	39.09	2.72	62.13	3.04
0.4	34.26	2.47	48.2	2.27
0.5	26.52	2.09	33.73	1.76
0.6	16.4	1.6	19.11	1.37
0.7	4.46	1.01	4.66	1.13
0.8	8.6	0.34	9.45	1.04
0.9	22.29	0.48	22.9	0.91

TABLE V. EFFECT OF 5% MISMATCHES IN TUNING CURRENTS FOR 600 MHz

$2 I_C$ (mA)	Soft coupling		Hard Coupling	
	Δf (MHz)	Phase error (°)	Δf (MHz)	Phase error (°)
0.1	36.34	10.82	5.81	7.86
0.2	27.96	5.47	5.94	4.03
0.3	16.77	3.65	5.46	3.35
0.4	4.41	2.71	8.69	2.09
0.5	9.29	2.21	10.49	1.74
0.6	24.13	1.88	12.17	1.43
0.7	39.66	1.71	14.03	1.2
0.8	55.85	1.47	15.63	1.05
0.9	72.04	1.52	17.33	0.96

TABLE VI. EFFECT OF 5% MISMATCHES IN TUNING CURRENTS (1.4 GHz)

$2 I_C$ (mA)	Soft coupling		Hard Coupling	
	Δf (MHz)	Phase error (°)	Δf (MHz)	Phase error (°)
0.1	No oscillation		No oscillation	
0.2			26.91	4.6
0.3	6.15	3.87	13.1	3.39
0.4	9.41	3.01	1.9	2.73
0.5	16.24	2.58	17.62	2.3
0.6	25.51	2.34	33.58	2.01
0.7	36.49	2.08	49.35	1.81
0.8	48.61	1.94	64.76	1.57
0.9	61.23	1.95	79.6	1.45

TABLE VII. EFFECT OF 1% MISMATCHES IN TUNING CURRENTS (600 MHz)

$2 I_C$ (mA)	Soft coupling		Hard Coupling	
	Δf (MHz)	Phase error (°)	Δf (MHz)	Phase error (°)
0.1	44.26	2.2	1.75	1.57
0.2	35.27	1.17	1.73	0.82
0.3	24.31	0.76	0.87	0.52
0.4	11.86	0.68	0.54	0.32
0.5	1.81	0.53	2.06	0.24
0.6	16.6	0.64	3.65	0.15
0.7	32.16	0.56	5.26	0.09
0.8	48.38	0.6	6.85	0.27
0.9	64.87	0.67	8.45	0.32

TABLE VIII. EFFECT OF 1% MISMATCHES IN TUNING CURRENTS 1.4 GHz

$2 I_C$ (mA)	Soft coupling		Hard Coupling	
	Δf (MHz)	Phase error (°)	Δf (MHz)	Phase error (°)
0.1	No oscillation		No oscillation	
0.2			40.04	1.91
0.3	7.65	2.49	26.46	1.43
0.4	3.85	1.98	11.79	1.17
0.5	3.31	1.79	3.49	0.97
0.6	12.92	1.59	18.98	0.87
0.7	24.32	1.57	34.38	0.81
0.8	36.91	1.55	49.3	0.73
0.9	50.12	1.52	63.74	0.57

TABLE IX. EFFECT OF 10% MISMATCHES IN TUNING CURRENTS (600 MHz)

$2 I_C$ (mA)	Soft coupling		Hard Coupling	
	Δf (MHz)	Phase error (°)	Δf (MHz)	Phase error (°)
0.1	24.29	23.23	15.73	15.93
0.2	17.79	10.86	15.82	8.42
0.3	7.18	7.11	17.28	5.79
0.4	5.12	5.27	19.17	4.42
0.5	18.67	4.33	21.16	3.64
0.6	33.31	3.62	23.19	2.95
0.7	48.75	3.03	25.13	2.59
0.8	64.73	2.72	27.04	2.32
0.9	80.69	2.53	28.73	1.97

TABLE X. EFFECT OF 10% MISMATCHES IN TUNING CURRENTS (1.4 GHz)

$2 I_C$ (mA)	Soft coupling		Hard Coupling	
	Δf (MHz)	Phase error (°)	Δf (MHz)	Phase error (°)
0.1	No oscillation		No oscillation	
0.2			10.92	8
0.3	22.66	5.92	3.18	5.83
0.4	25.24	4.51	18.61	4.66
0.5	31.63	3.81	34.84	3.95
0.6	40.43	3.21	51.33	3.44
0.7	50.89	2.85	67.72	3.06
0.8	62.36	2.65	83.78	2.77
0.9	74.4	2.41	99.11	2.42

A larger mismatch requires a larger coupling current to establish synchronous operation (locking), but this leads to a much increased phase error. This error may be reduced by further increasing the coupling current, but this influences the frequency.

Simulations show that the coupling current should be increased when the tuning currents are mismatched, since the phase error is reduced with increase of the coupling current. The phase error is lower for “hard” than for “soft” coupling. The “hard” coupling provides a significant lower quadrature error and allows higher coupling currents without stopping the oscillations. In comparison with the results presented in [7] the proposed circuits exhibits a lower phase error, assuming the same coupling current, i.e. 0.5mA.

V. FREQUENCY LOCKING

We also investigated frequency locking at a sub-harmonic frequency when an external current source is applied between points B and B₁ (see Fig. 1b). The oscillator at 600 MHz can be synchronized by a current source with 100 μA of amplitude, as shown in Fig. 9.

It should be noted that locking is observed only for odd harmonics, since the multivibrator output signal has odd symmetry, and, therefore, has odd harmonics only.

We injected a locking signal in the oscillator running at the frequency of 600 MHz. It was possible to lock the oscillator up to the 11th sub-harmonic frequency. Fig. 10 shows the free running oscillations (up to 10 ns) and the application of locking signal after 10 ns. It is seen that the multivibrators are locked in just 2 periods. This is an advantage of multivibrators: they have short transients, and therefore, they can adjust the frequency in one or two periods. This is one reason (sometimes neglected) why RC oscillators survive. The LC oscillators would have long transients and they need, in some cases, hundreds of periods to adjust the oscillation frequency. Similar results are obtained for the free-running frequency of 1.4 GHz, but, the maximum sub-harmonic frequency to lock the oscillator is the 5th.

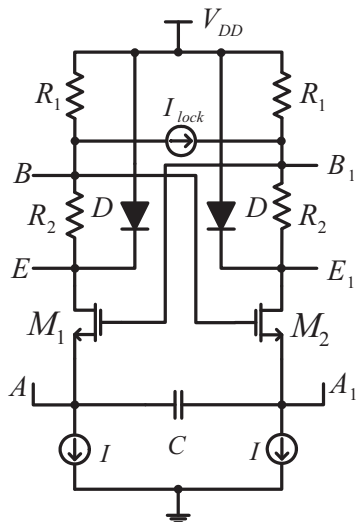


Figure 9. Sub-harmonic injection-locked multivibrator.

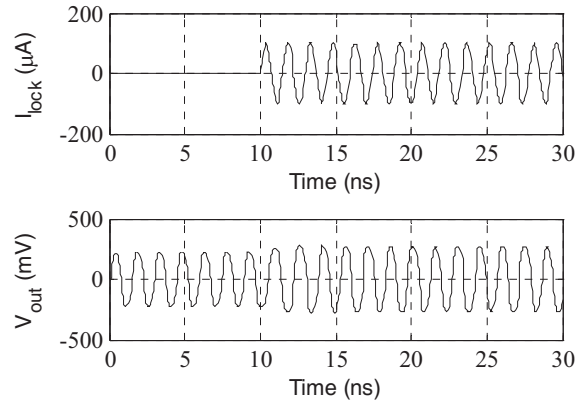


Figure 10. Waveforms for the injection locking.

We also investigated the locking range of the single multivibrator for a particular harmonic. For example, the oscillator does not lock with a frequency lower than 550 MHz, and higher than 860 MHz for the first harmonic. With higher harmonics the oscillator will have lower locking range, as shown in Table XI.

Considering two coupled multivibrators and injecting a current in one of them, the locking range is much smaller, as it is also shown in Table XI. This locking is possible only if the injection current is higher than the coupling current (in the presented case $I_C = 500 \mu A$) and one can only synchronize the system up to the 5th harmonic. For 1.4 GHz the locking range goes to the 7th (as shown in Table XII).

With a mismatch of 5 % in currents I , one can lock the oscillator with an external signal of frequency (3.379 GHz) up to 5 times the free-running frequency (about 600 MHz), as shown on Table XIII. This frequency ratio is reduced to 3 if we increase the mismatch to 10 % (2.027 GHz). Thus, the frequency ratio and the locking range are reduced when there are mismatches in bias currents. Mismatches in capacitors have the same effect.

TABLE XI. OSCILLATOR LOCKING RANGE

Harmonic number	Single Oscillator		Coupled Oscillators	
	Low freq. (GHz)	High freq. (GHz)	Low freq. (GHz)	High freq. (GHz)
1	0.55	0.86	0.46	0.75
3	1.85	2.2	1.7	2.1
5	3.33	3.45	3.04	3.33
7	4.73	4.75	-	-
9	6.079	6.1	-	-
11	7.4345	7.44	-	-

TABLE XII. OSCILLATOR LOCKING RANGE 1.4 GHz

Harmonic number	Coupled Oscillators	
	Low freq. (GHz)	High freq. (GHz)
1	1.1	1.65
3	3.8	4.2
5	6.7	6.8
7	9.45	9.48
9	-	-

TABLE XIII. OSCILLATOR LOCKING WITH MISMATCH

Harmonic number	Single Oscillator			
	Mismatch 5%		Mismatch 10%	
	Low freq. (GHz)	High freq. (GHz)	Low freq. (GHz)	High freq. (GHz)
1	0.56	0.86	0.57	0.88
3	1.88	2.2	1.95	2.2
5	3.38	3.45	-	-
7	-	-	-	-

Simulation results with external locking show that the multivibrators in Fig. 2 do not necessarily run at the same frequency. The multivibrator of lower frequency can be in lock with a multivibrator running at a higher frequency, and the locking has the properties similar to the locking at an external synchronizing source.

VI. DISCUSSION AND CONCLUSIONS

The simulation results show that using the proposed low area and low cost oscillator circuit, we can cover the frequency range required for WMTS applications.

The proposed oscillator has three degrees of freedom to control the oscillation frequency: the timing capacitance, the gate voltage (which depends on the resistor divider ratio), and the tuning current. These can be used to maximize the tuning range, to alter the shape of the tuning characteristic and to move it to a desirable range. The same degrees of freedom are preserved when two oscillators are coupled to obtain a quadrature oscillator.

Simulations in a 130 nm CMOS technology show that the quadrature oscillator is very robust with respect to mismatches of timing capacitors and of charging currents, especially with “hard coupling”. The frequency tuning range is from 450 MHz to about 1 GHz, covering the 600 MHz band. By reducing the capacitor value (this can be done using a varactor and/or a discrete control), the tuning range becomes 1 GHz to 2 GHz for “hard” coupling, thus, covering the 1.4 GHz band. These bands are required for biomedical applications.

We are unable, at the present time, to explain why the oscillations stop at higher frequencies. This problem requires further investigation.

The circuit presented in this paper can be synchronized by an external current with a frequency that is an odd multiple of the oscillation frequency. This synchronization can be applied to one of the two multivibrators in the quadrature oscillator. The synchronization transient is fast, and synchronized oscillation is set in a few periods. This sub-harmonic locking can be useful in design of PLL frequency dividers.

REFERENCES

- [1] Luis B. Oliveira, J. Fernandes, Chris Verhoeven, Igor Filanovsky, and Manuel Silva, *Analysis and Design of Quadrature Oscillators*, Springer, 2008.
- [2] J. Fernandes, M. Kouwenhoven, C. van den Bos, L. B. Oliveira, C. J. M. Verhoeven, “The Effect of Mismatches and Delay on the Quadrature Error of a Cross-Coupled Relaxation Oscillator”, *IEEE Trans. Circuits and Systems – I*, vol. 54, pp. 2592-2598, December 2007.
- [3] L. Romanò, S. Levantino, A. Bonfanti, C. Samori and A. L. Lacaita “Multiphase LC oscillators”, *IEEE Trans. Circuits and Systems – I*, vol. 53, n°7, pp. 1579-1588, July 2006.
- [4] L. Jia, J. Ma, K. S. Yeo, and M. Do, “9.3 – 10.4 GHz Band Cross-Coupled Complementary Oscillator with Low Phase-Noise Performance”, *IEEE Transactions on Microwave Theory and Techniques*, vol. 52, n° 4, pp. 1273 – 1278, April 2004.
- [5] J. Tang, D. Kasperkovitz, and A. van Roermund, “A 9.8 – 11.5 GHz Quadrature Ring Oscillator for Optical Receivers”, *IEEE J. Solid-State Circ.*, vol. 27, pp. 438 - 442, March 2002.
- [6] A. Allam, I. M. Filanovsky, L. B. Oliveira and J. R. Fernandes, “Synchronization of Mutually Coupled LC-Oscillators”, *IEEE Int. Symp. Circuits and Systems (ISCAS’06)*, pp. 4297-4300, May 2006.
- [7] L. B. Oliveira, A. Allam, I. M. Filanovsky, J. Fernandes, C. J. M. Verhoeven, and Manuel Silva, “Experimental Comparison of Phase Noise in Cross-Coupled RC- and LC-Oscillators”, *International Journal on Circuit Theory and Applications*, Wiley InterScience, published online April 2009.
- [8] Krzysztof Iniewski, *VLSI Circuits for Biomedical Applications*, chap. 5, Artech House, 2008.
- [9] P.R. Gray, P. J. Hurst, S.H. Lewis, and R.G. Meyer, *Analysis and Design of Analog Integrated Circuits*, 4th ed., J. Wiley, New York, 2007.
- [10] A. Buonomo, A. Lo Schiavo, “Analysis of Emitter (Source)-Coupled Multivibrators”, *IEEE Trans. Circuits and Systems-I*, vol. 53, no. 6, pp. 1193-1202, 2006.
- [11] I.M. Filanovsky, C.J.M. Verhoeven, “Sinusoidal and Relaxation Oscillations in Source-Coupled Multivibrators”, *IEEE Trans. Circuits and Systems-II*, vol. 54, no. 11, pp. 1009-10013, 2007.
- [12] C.J.M. Verhoeven, “A High-Frequency Electronically Tunable Quadrature Oscillator”, *IEEE J. Solid-State Circuits*, vol. 27, no. 7, pp. 1097-1100, 1992.
- [13] B. Gilbert, “A Versatile Monolithic Voltage-to-Frequency converter”, *IEEE J. Solid-State Circuits*, vol. SC-11, no. 6, pp. 852-864, 1976.
- [14] Igor M. Filanovsky, Luis B. Oliveira, and Jorge Fernandes, “Wide Tuning Range Quadrature VCO Using Coupled Multivibrators”, *Electronics and Telecommunications Quarterly*, vol. 55, n° 4, pp.53-68, 2009.
- [15] I.M. Filanovsky, “Remarks on Design of Emitter-Coupled Multivibrators”, *IEEE Trans. Circuits and Systems*, vol. 35 no. 6, pp. 1182-11185, 1992.
- [16] L. B. Oliveira, I. M. Filanovsky, and C. J. M. Verhoeven, “Exact Calculations of Amplitudes and Frequency in an RC Oscillator with Quadrature Outputs”, *47th IEEE Int. Midwest Symp. Circuits and Systems (MWSCAS’04)*, vol. I, pp.413-416, July 2004.



João Carlos F. A. Casaleiro was born in Setúbal, Portugal, on November 17, 1977. He received the B.Sc. degree from Instituto Superior de Engenharia de Lisboa (ISEL), Portugal, in 2001.

He joined the Departamento de Engenharia de Electrónica, Telecomunicações e Computadores, Instituto Superior de Engenharia de Lisboa (ISEL), Lisbon, in 2004, as an Assistant Professor.

He is currently working toward the Ph.D. degree in Departamento de Engenharia Electrotécnica (DEE), Faculdade de Ciências e Tecnologia (FCT), Universidade Nova de Lisboa (UNL). His research interests include integrated CMOS receivers, oscillators and mixers.



Hugo Lopes was born in Alcântara, Lisboa, in 1986. He received the M.Sc. degree in electrical engineering from the Faculdade de Ciências e Tecnologia of the Universidade Nova de Lisboa (FCT/UNL), Lisboa, Portugal, in 2010. His scientific interests are in the design of modern RF architectures using CMOS technology.



Luís B. Oliveira (S'02–M'07) was born in Lisbon, Portugal, in 1979. He graduated in electrical and computer engineering and obtained the Ph.D. degree from Instituto Superior Técnico (IST), Technical University of Lisbon, in 2002 and 2007 respectively. Since 2001 he has been a member of the Analog and Mixed Signal Circuits Group at INESC-ID. Although his research work has been done mainly at INESC-ID, he has had intense collaboration with

TU Delft, in The Netherlands, and University of Alberta, in Canada. In 2007, he joined the teaching staff of the Department of Electrical Engineering of Faculty of Sciences and Technology, Universidade Nova de Lisboa (UNL), and is currently a researcher at CTS-UNINOVA. His current research interests are on RF oscillators, mixers, and other building blocks for RF integrated transceivers.

Prof. Oliveira has several publications in international journals and leading conferences and he is co-author of "Analysis and Design of Quadrature Oscillators" (Springer, 2008).



I. M. Filanovsky (M'81–SM'90) was born in Kirov, USSR, in 1940. He received the M.Sc. degree in 1962 and the Ph.D. degree in 1968, both in electrical engineering from V. I. Ulianov (Lenin) Institute of Electrical Engineering, Leningrad, USSR.

In 1976, he joined the University of Alberta, Canada, where he is currently a Professor Emeritus. Dr. I. M. Filanovsky is the author or coauthor of 9 books and about 300 journal and conference papers on circuit theory (theory of approximation, theory and technical applications of oscillations, strongly nonlinear

oscillations), and applied microelectronics (analog electronic circuits, oscillators and multivibrators, signal-conditioning circuits for sensors). He has four patents on electronic circuits. His paper "A 100 dB CMRR CMOS Operational Amplifier with Single-Supply Capability", co-authors V. Ivanov and Junlin Zhou, obtained "The Best Paper Award" at the International Conference on Electronics, Circuits and Systems, ICECS2004, Tel-Aviv, Israel.

Dr. I. M. Filanovsky is currently an Associated Editor of IEEE Transactions on Circuits and Systems (Part I) and Associated Editor of International Journal of Circuit Theory and Applications.